

# Molecular Evolution of the Yap/Yorkie Proto-Oncogene and Elucidation of Its Core Transcriptional Program

Aissam Ikmi,<sup>1</sup> Bjoern Gaertner,<sup>1</sup> Christopher Seidel,<sup>1</sup> Mansi Srivastava,<sup>2</sup> Julia Zeitlinger,<sup>1,3</sup> and Matthew C. Gibson<sup>\*1,4</sup>

<sup>1</sup>Stowers Institute for Medical Research, Kansas City, MO

<sup>2</sup>Whitehead Institute for Biomedical Research, Cambridge, MA

<sup>3</sup>Department of Pathology and Laboratory Medicine, University of Kansas School of Medicine, Kansas City, KS

<sup>4</sup>Department of Anatomy and Cell Biology, University of Kansas School of Medicine, Kansas City, KS

\*Corresponding author: E-mail: MG2@stowers.org.

Associate editor: Stuart Newfeld

## Abstract

Throughout Metazoa, developmental processes are controlled by a surprisingly limited number of conserved signaling pathways. Precisely how these signaling cassettes were assembled in early animal evolution remains poorly understood, as do the molecular transitions that potentiated the acquisition of their myriad developmental functions. Here we analyze the molecular evolution of the proto-oncogene *yes-associated protein* (Yap)/Yorkie, a key effector of the Hippo signaling pathway that controls organ size in both *Drosophila* and mammals. Based on heterologous functional analysis of evolutionarily distant Yap/Yorkie orthologs, we demonstrate that a structurally distinct interaction interface between Yap/Yorkie and its partner TEAD/Scalloped became fixed in the eumetazoan common ancestor. We then combine transcriptional profiling of tissues expressing phylogenetically diverse forms of Yap/Yorkie with ChIP-seq validation to identify a common downstream gene expression program underlying the control of tissue growth in *Drosophila*. Intriguingly, a subset of the newly identified Yorkie target genes are also induced by Yap in mammalian tissues, thus revealing a conserved Yap-dependent gene expression signature likely to mediate organ size control throughout bilaterian animals. Combined, these experiments provide new mechanistic insights while revealing the ancient evolutionary history of Hippo signaling.

**Key words:** Yap, growth control, target genes, Metazoa, evolution.

## Introduction

Recent advances in comparative genomics have potentiated new insights into the evolution of animal multicellularity (Putnam et al. 2007; King et al. 2008; Srivastava et al. 2008, 2010), with a primary focus on molecules that maintain stable cell–cell interactions and cell differentiation (King et al. 2003; Nichols et al. 2006; Abedin and King 2008; Larroux et al. 2008; Sebe-Pedros et al. 2010). Although these fundamental processes are essential to form an epithelium composed of different cell types, the evolution of animal complexity must have also required the incorporation of novel tissue growth-regulatory mechanisms. In both insects and mammals, the Hippo tumor suppressor pathway serves such a function by antagonizing the growth-promoting activity of a transcriptional coactivator known as Yorkie (Yki) in *Drosophila* and *yes-associated protein* (Yap) in mammals (Dong et al. 2007; Oh and Irvine 2010; Zhao et al. 2010). Importantly, consistent with its function in control of tissue growth, Yap is a candidate oncogene in human disease (Overholtzer et al. 2006; Zender et al. 2006). In addition, several lines of evidence suggest that Yap also plays a critical role in other biological processes, including cell fate determination, stem cell proliferation, and regeneration (Zhao et al. 2011; Liu et al. 2012).

At the molecular level, Yap contains multiple functional domains, including TEAD-binding (TBD), WW, coiled-coil, and PDZ-binding motifs (Wang et al. 2009). To promote growth, Yap interacts with Scalloped/TEAD and other DNA-binding partners to drive the expression of cell cycle regulators and cell death inhibitors (Huang et al. 2005; Goulev et al. 2008; Wu et al. 2008; Zhang, Ren, et al. 2008; Zhao et al. 2008; Peng et al. 2009; Oh and Irvine 2011). These interactions require Yap's TBD and WW motifs (Zhao et al. 2009; Zhang, Milton, et al. 2009). The growth-promoting activity of Yap is in turn constrained through phosphorylation by Warts/Lats (Huang et al. 2005; Dong et al. 2007), a member of an ancient eukaryotic kinase cassette including Hippo/Mst (Sebe-Pedros et al. 2012). Yap phosphorylation induces cytoplasmic retention by recruiting 14-3-3 proteins (Camargo et al. 2007; Dong et al. 2007; Zhao et al. 2007), which then limit the ability of Yki/Yap to complex with its DNA-binding partners.

Recently, the identification and functional analysis of Yap and TEAD from the amoeba *Capsaspora owczarzaki* suggests that the capacity to control tissue growth may have emerged through co-option of a preexisting Hippo-Yap regulatory architecture. However, unlike Human Yap, the *Capsaspora* ortholog alone is not sufficient to induce tissue overgrowth in *Drosophila* (Dong et al. 2007; Sebe-Pedros et al. 2012).

© The Author 2014. Published by Oxford University Press on behalf of the Society for Molecular Biology and Evolution.

This is an Open Access article distributed under the terms of the Creative Commons Attribution Non-Commercial License (<http://creativecommons.org/licenses/by-nc/3.0/>), which permits non-commercial re-use, distribution, and reproduction in any medium, provided the original work is properly cited. For commercial re-use, please contact [journals.permissions@oup.com](mailto:journals.permissions@oup.com)

Open Access

This raises the question of how and when the Yap-TBD changed during evolution. Here, we compare the structure of the TBD from phylogenetically informative lineages including multiple early branching metazoan species, as well as the closest unicellular relatives of Metazoa. We then use a heterologous expression assay to 1) directly compare the growth-promoting activity of divergent Yap orthologs and 2) identify a downstream transcriptional profile induced by select variants in the *Drosophila* eye disc. Combined, these results demonstrate that the Yap-TEAD interaction interface became stabilized sometime after the divergence of sponges from the eumetazoan common ancestor. In addition, coupled with Chip-seq validation of Yki/Scalloped binding sites, our comparative analysis identifies multiple novel Yap/TEAD targets in *Drosophila* while hinting at the existence of a conserved bilaterian gene expression program downstream of Yap/TEAD.

## Results

### Evolutionary Changes in Yap/Yki Protein Architecture

To determine the extent to which the structural features of Yap are conserved between animals and their unicellular relatives, we performed a detailed domain composition analysis of Yap orthologs from species occupying key phylogenetic positions (fig. 1A). In addition to *Drosophila* and *Homo*, these included the cnidarian *Nematostella vectensis*, the placozoan *Trichoplax adhaerens* and the demosponge *Amphimedon queenslandica*, which are modern representatives of the earliest branching Metazoa (Putnam et al. 2007; Srivastava et al. 2008, 2010). We also analyzed the domain structure of Yap orthologs from the genome of three nonmetazoan species, the amoeba *C. owczarzaki*, and the choanoflagellates *Monosiga brevicollis* and *Salpingoeca rosetta* (King et al. 2008; Suga et al. 2013). Consistent with prior findings (Sebe-Pedros et al. 2012), our phylogenetic analyses showed a well-supported monophyletic group that included the known bilaterian Yap protein together with a single putative Yap protein from each analyzed genome (supplementary fig. S1, Supplementary Material online). This contrasts with vertebrate genomes, which contain a paralogous copy of Yap (Taz), proposed to have originated from a gene duplication event early in vertebrate evolution (Hilman and Gat 2011).

Interestingly, the most critical Lats/Warts phosphorylation site in Yap (corresponding to Ser127 in *Homo*) was conserved in all metazoan species analyzed (fig. 1B). It was also present in the *Monosiga*, *Salpingoeca*, and *Capsaspora* Yap proteins, although the associated regulatory 14-3-3 binding motif was incomplete (fig. 1B). These observations are consistent with conservation of the Yap-Lats regulatory interaction throughout animal evolution.

As expected, the Yap orthologs we identified shared many additional features. However, they also displayed some critical structural variations. Most prominently, these included alterations in the architecture of the TBD (fig. 1A and supplementary fig. S2, Supplementary Material online). Although the TBD  $\alpha$ 1-loop- $\alpha$ 2 secondary structure (Chen et al. 2010; Li

et al. 2010) was conserved in Eumetazoa, this protein-protein interaction domain diverged in *Amphimedon*, exhibiting an additional  $\alpha$ 3 helix motif (fig. 1C and D). Beyond metazoans, the most conspicuous conserved motifs were the Yap WW and coiled-coil domains (fig. 1A), indicating that this structural combination was found in the unicellular ancestors of animals. Intriguingly, we manually identified  $\alpha$ 1 and  $\alpha$ 2 helix motifs as a cryptic TBD in the N-terminus of *Capsaspora* Yap (fig. 1C and D). This may represent a transitional state that existed before evolution of the complete  $\alpha$ 1-loop- $\alpha$ 2 structure in Eumetazoa. In addition, a highly divergent Yap TBD containing only the  $\alpha$ 1 helix motif was found in *Monosiga* (fig. 1D). Combined, these results suggest a remarkable structural plasticity of the TBD during early Yap evolution, followed by fixation of the  $\alpha$ 1-loop- $\alpha$ 2 structure throughout Eumetazoa.

### Heterologous Functional Analysis of Yap/Yki Orthologs in *Drosophila*

We next set out to determine the functional implications of the evolutionary changes in Yap protein architecture. Because experimental tools are a limiting factor in most nonmodel organisms, we took advantage of *Drosophila* genetics to directly compare the activities of representative Yap orthologs in a uniform in vivo system. We first generated transgenic flies carrying inducible forms of yap from *Monosiga*, *Amphimedon*, *Trichoplax*, and *Nematostella*, as well as inducible forms of *Drosophila* yki and *Homo* yap for experimental controls. The phiC31-attP-attB site-specific integration technique was employed to insert all transgenes into a specific genomic site, ensuring identical transgene expression levels (Groth et al. 2004; Bischof et al. 2007). Because Yap activity is regulated by Lats/Warts phosphorylation, we also generated hypothetically nonphosphorylatable forms of each Yap ortholog by modifying the appropriate serine residues to create constitutively active Yap variants (fig. 2A). Although the mutated serine for each metazoan Yap matched the position of the critical phosphorylation site of Yki/Yap (Ser168/127), the only candidate residue within an optimal 14-3-3 binding motif for the *Monosiga* protein was Ser48.

Yki/Yap misexpression is sufficient to induce tissue overgrowth in *Drosophila* (Huang et al. 2005; Dong et al. 2007). We therefore performed a heterologous overexpression assay to compare the activity of each Yap ortholog in the *Drosophila* eye, using Glass Multiple Reporter-Gal4 (GMR-Gal4) to drive tissue-specific expression. Contrasting with the effects of *Monosiga* Yap, the *Amphimedon*, *Trichoplax*, and *Nematostella* variants elicited distinct degrees of overgrowth (fig. 2A and B). Importantly, each of these orthologs exhibited roughly equivalent protein stability in *Drosophila* S2 cells, indicating that the observed phenotypic variability arose from protein-intrinsic properties (fig. 2C). *Trichoplax* Yap produced an exceptionally severe overgrowth phenotype with enlarged, folded adult eyes. This effect was even further enhanced in animals overexpressing *Trichoplax* Yap<sup>S81A</sup> (fig. 2A and B). We also found evidence for phosphoregulation of Yap from *Amphimedon* and *Nematostella*; both showed similar

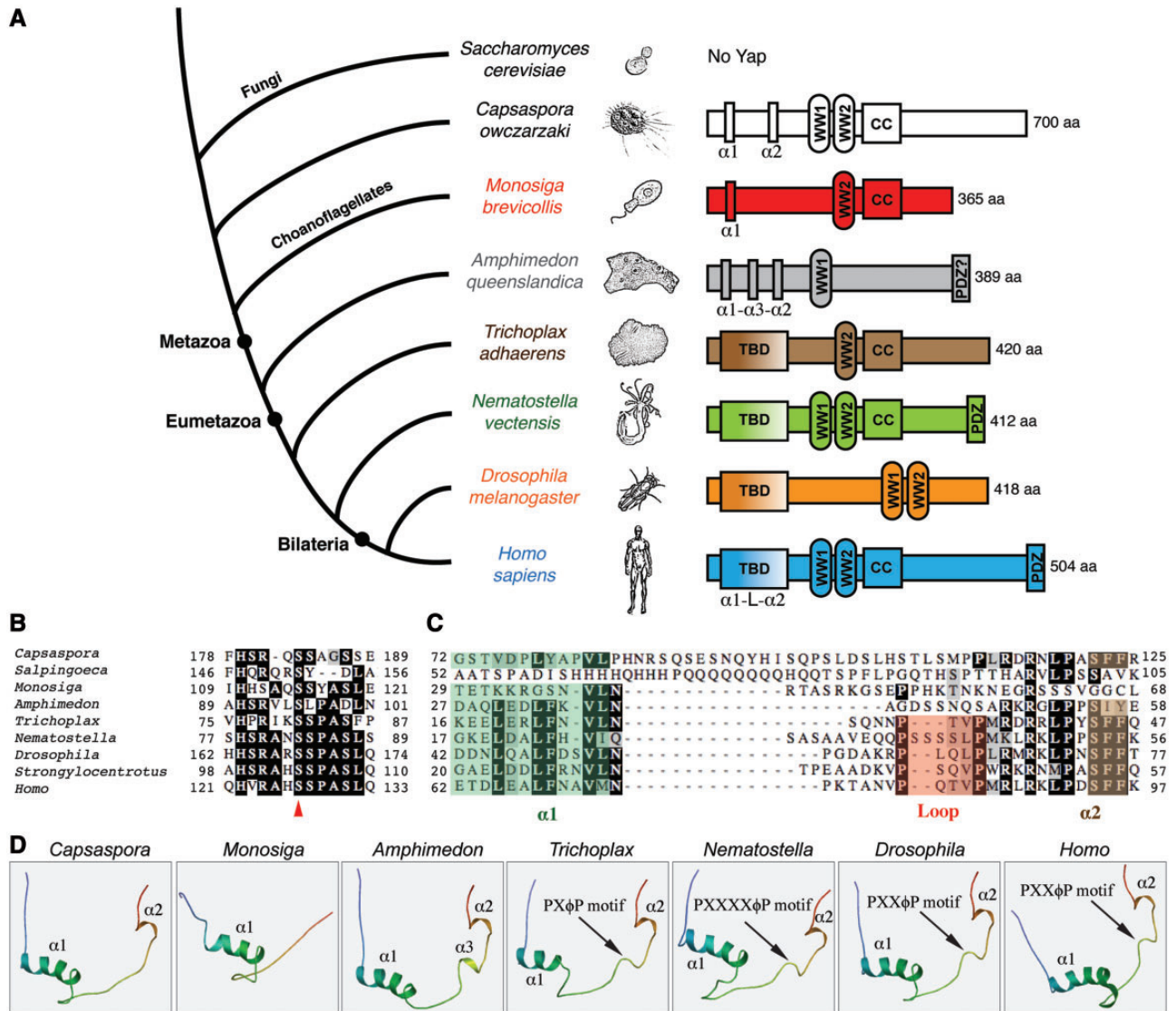


**Fig. 1.** Domain architecture of evolutionary distant Yap orthologs. (A) A simplified metazoan phylogeny including the unicellular species *Monosiga brevicollis*, *Capsaspora owczarzaki*, and *Saccharomyces cerevisiae*. Domain composition and protein size for each Yap ortholog are indicated. The annotated domains include the TBD, which indicates a complete TEAD binding domain containing two short helices ( $\alpha 1$  and  $\alpha 2$ ) and a loop (L) in between. This protein interaction domain is divergent in *Amphimedon*, *Monosiga*, and *Capsaspora*. Also indicated are the WW1 and WW2 domains (WW), coiled-coil domains (C-C), and the PDZ binding motif. (B) The most critical phosphorylation site of Yap (red arrowhead) is conserved in all indicated species. The HXRXXS motif associated with this site is incomplete in *Monosiga* and *Capsaspora*. (C) Alignments of the N-terminal regions of Yap orthologs. Secondary structural elements are labeled as following:  $\alpha 1$  helix (green), loop (red), and  $\alpha 2$  helix (brown). The complete  $\alpha 1$ -loop- $\alpha 2$  TBD is conserved from placozoans to humans. (D) Predicted 3D structures of five metazoan Yap TBDs as well as two nonmetazoan Yap TBDs. The *Monosiga* TBD lacks both the loop and  $\alpha 2$  helix, while the *Capsaspora* is missing only the loop. The *Amphimedon* TBD possesses an additional helix ( $\alpha 3$ ) instead of a loop. The loop-containing motif is shorter in *Trichoplax* (PX $\phi$ P) but longer in *Nematostella* (PXXXX $\phi$ P), when compared with that of *Drosophila* and human (PXX $\phi$ P). X: any residue;  $\phi$ : hydrophobic residue; P: proline.

increases in eye size that were enhanced by mutation of the conserved phosphorylation sites (fig. 2A and B). Together, these results not only show that basal metazoan versions of Yap possess potent growth-promoting activity in *Drosophila* but also that they are regulated by phosphorylation via similar mechanisms to those of *Drosophila* Yki and human Yap. This implies that the Hippo/Wts cassette may function similar to phosphoregulate Yap in early branching metazoans. Consistent with this, we cloned a Warts/Lats ortholog from *Nematostella* and found that it was sufficient to rescue the corresponding *Drosophila* mutant, presumably through

phosphorylation of *Drosophila* Yki (supplementary fig. S3, Supplementary Material online).

Surprisingly, in contrast to the metazoan Yaps, overexpression of *Monosiga* Yap or its phosphomutant form resulted in significantly reduced eye size (fig. 2A and B). Although the proximal cause of this reduced eye phenotype is still unknown, cell clones overexpressing *Monosiga* Yap exhibited normal growth and morphology (data not shown). These findings exclude the possibility that *Monosiga* Yap acts as a dominant negative to inhibit cell proliferation through effects on endogenous Yki activity.

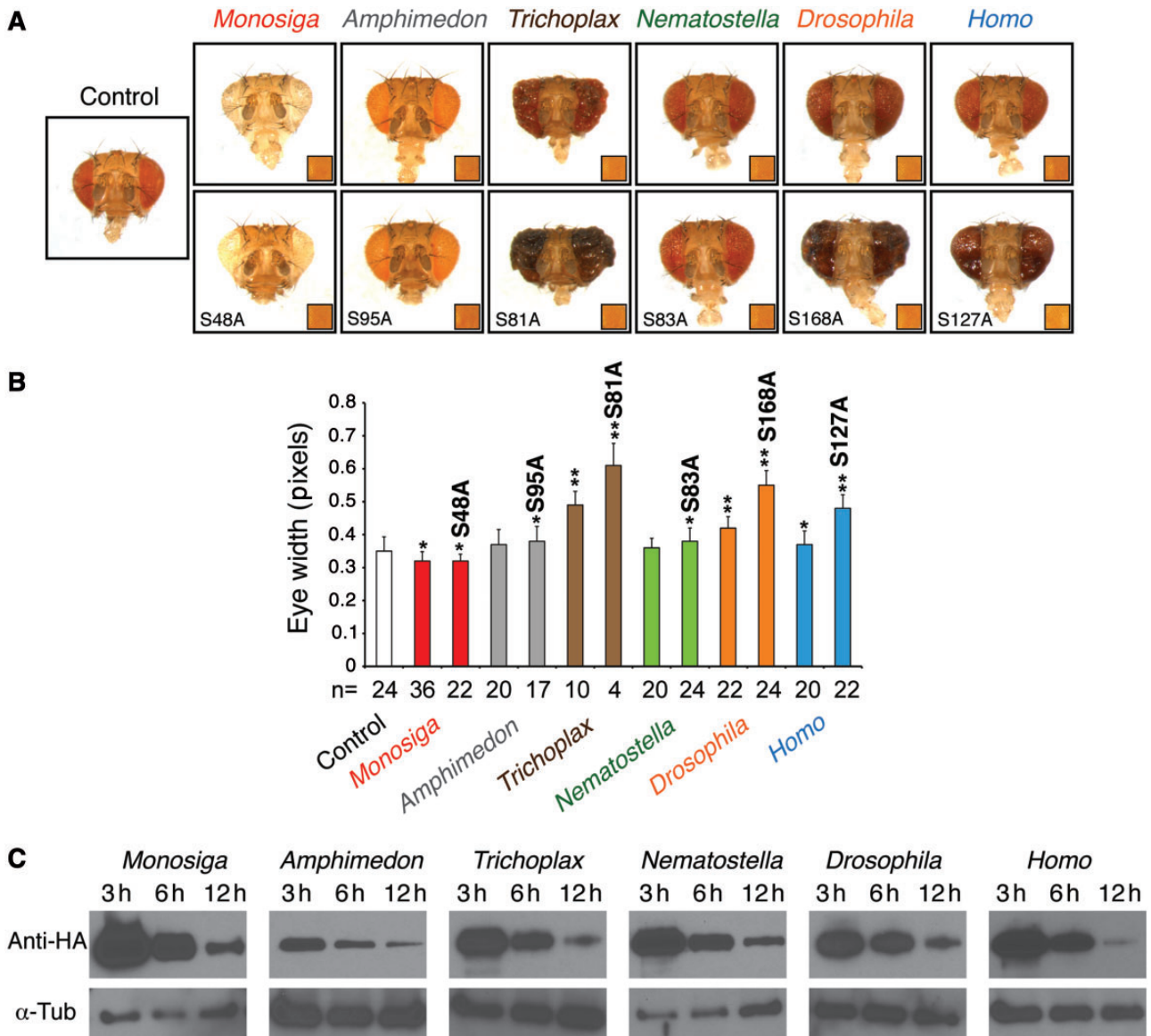


**Fig. 2.** In vivo functional analysis of Yap orthologs in *Drosophila*. (A) Representative adult female heads from flies overexpressing either *wild-type* (top row) or phosphomutant (bottom row) forms of the indicated Yap orthologs under the control of *GMR-Gal4*. Control is *GMR-Gal4/+*. Besides differences in eye size, we also observed changes in eye pigmentation, although the flies carrying each *UAS-transgene* originally displayed a similar eye color (inset boxes). (B) Quantification of adult eye widths for each overexpression condition. Statistical analysis was performed using a Student's *t*-test ( $n$  = number of analyzed adult eyes; \* $P < 0.05$ ; \*\* $P < 0.01$ ). (C) Constructs encoding C-terminal HA fusion proteins of each Yap ortholog were transfected into *Drosophila* S2 cells and expressed under the control of a heat-shock promoter. After heat shock, cell lysates were collected at the indicated times. Anti-HA western blots were used to show the protein levels of each Yap ortholog. Anti- $\alpha$ -tubulin was used as a loading control.

### Cellular and Molecular Basis for Yap/Yki Ortholog-Induced Overgrowth

To determine the cellular basis for eye size increases induced by each Yap ortholog, we next performed EdU incorporation assays to directly measure cell proliferation. As expected from our analysis of adult eye size, *Trichoplax* Yap<sup>S81A</sup> induced the most extensive cell proliferation in the *GMR-Gal4* domain (fig. 3A). As a consequence of this dramatic overgrowth, the eye disc epithelium was extensively folded and disorganized (fig. 3D and E). *Nematostella* Yap<sup>S83A</sup> induced significant but moderate ectopic cell proliferation when compared with *Drosophila* Yki<sup>S168A</sup> and

human Yap<sup>S127A</sup> (fig. 3A), resulting in extra bristles and interommatidial cells (IOCs) in the adult eyes (fig. 3D and E). Consistent with a Yki-like transcriptional output of *Trichoplax* and *Nematostella* Yap, both induced expression of Cyclin E and the cell death inhibitor *diap1* (fig. 3B, C, and C'). These findings show that *Nematostella* and *Trichoplax* Yap are able to induce cell proliferation and survival, behaving like their *Drosophila* and human counterparts.

Contrasting with their eumetazoan counterparts, *Amphimedon* Yap<sup>S95A</sup> and *Monosiga* Yap<sup>S48A</sup> did not induce Cyclin E, *diap1*, or cell proliferation as indicated by EdU incorporation (fig. 3A, B, C, and C'). Further, overgrowth

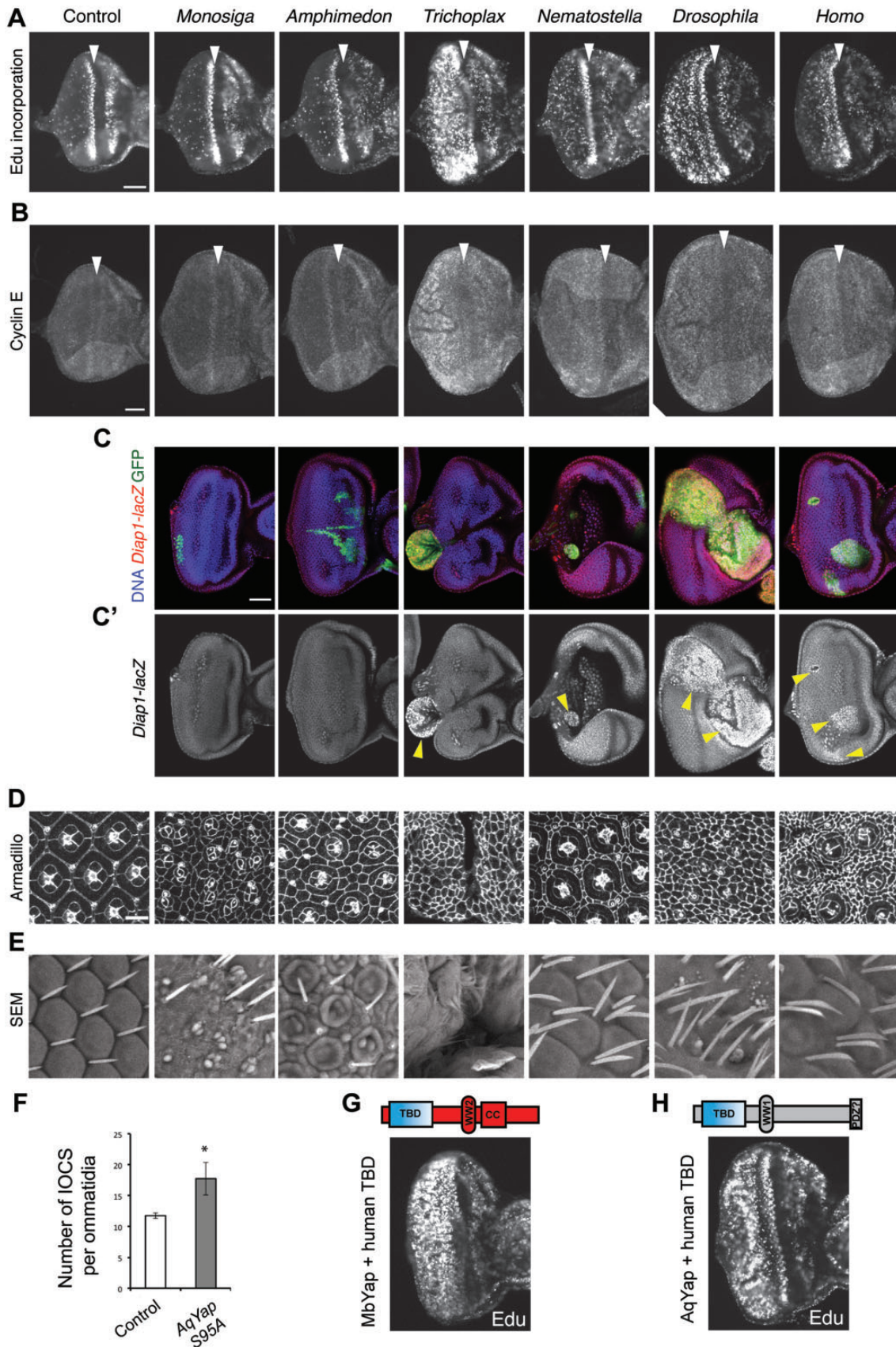


**FIG. 3.** Cellular and molecular mechanisms underlying Yap ortholog-induced overgrowth in *Drosophila*. (A) Edu labeling in eye discs overexpressing hypothetically nonphosphorylatable forms of Yap from the indicated species under the control of *GMR-Gal4*. Note the dramatic induction of proliferation by *Trichoplax yap* and the absence of ectopic proliferation caused by the *Monosiga* and *Amphimedon* orthologs. (B) Immunostaining of Cyclin E in eye discs of the same genotypes indicated above. Arrowheads indicate the position of the morphogenetic furrow.

(continued)

was not induced following misexpression in other imaginal discs (data not shown). Intriguingly, pupal retinæ of *GMR-Gal4>Amphimedon Yap<sup>S95A</sup>* animals exhibited an elevated number of IOCs, which are normally eliminated by developmentally programmed apoptosis (fig. 3D and F) (Wolff and Ready 1991). Following expression of *Amphimedon Yap<sup>S95A</sup>*, these cells failed to undergo normal differentiation of the lens cuticle and retained a pupal-like appearance in adult animals (fig. 3E). More pronounced defects in the differentiation and patterning of ommatidial cells were observed in retinæ overexpressing *Monosiga Yap*, as the normal hexagonal topology of ommatidial subunits was abolished (fig. 3D and E). These results suggest a defect in retinal differentiation and are consistent with severe reductions of eye pigmentation observed in flies overexpressing *Monosiga* and *Amphimedon* proteins (fig. 2A).

The *Amphimedon* and *Monosiga Yap* proteins both possessed an incomplete  $\alpha$ 1-loop- $\alpha$ 2 TBD (fig. 1C), and thus their inability to drive proliferative growth was most likely due to a failure to recognize the endogenous *Drosophila* TEAD (Scalloped, Sd). To test this hypothesis, we first constructed chimeric forms of *Amphimedon* and *Monosiga Yap* bearing the 50-amino acid human TBD. Strikingly, in both cases, this single change in protein architecture was sufficient to induce extensive ectopic proliferation in the eye disc (fig. 3G and H). Second, we found that *Amphimedon Yap* was able to form a functional protein complex with *Amphimedon* TEAD in *Drosophila* S2 cells (supplementary fig. S4, Supplementary Material online). In parallel, as expected from our in vivo heterologous expression assay, we did not detect a physical interaction between *Amphimedon Yap* and *Drosophila* Sd (supplementary fig. S4, Supplementary Material online), despite the fact that TEAD proteins exhibit few differences in their Yap-binding interfaces (supplementary fig. S5, Supplementary Material online). These findings suggest a critical functional divergence in Yap-TEAD pairwise interactions during early animal evolution. Consistent with this scenario, *Capsaspora Yap* cannot induce tissue overgrowth in *Drosophila* unless it is co-overexpressed with the endogenous *Capsaspora* TEAD (Sebe-Pedros et al. 2012). In contrast to the *Amphimedon Yap*, *Nematostella Yap* was able to physically interact with both *Nematostella* TEAD and *Drosophila* Sd (supplementary fig. S4A, Supplementary Material online). Thus, these findings not only show the deep evolutionary origins of Yap-TEAD activity but also reveal that the interaction interface between Yap and TEAD changed during early metazoan evolution and ultimately became fixed in

eumetazoan Yap proteins. Although the evolutionary advantages of this modification remain unknown, we speculate that it may have served as an important adaptation of Yap to critical new roles in the growth control in the multicellular context.

### The Transcriptional Output of Yap/Yki Orthologs in *Drosophila*

In vivo, Yap acts through modulation of target gene expression (Overholtzer et al. 2006; Dong et al. 2007; Hao et al. 2008; Lu et al. 2010). To leverage the evolutionary diversity of selected Yki/Yap orthologs and identify novel transcriptional targets of the Hippo pathway in *Drosophila*, we performed RNA sequencing analysis (RNA-seq) on total RNA isolated from *GMR-Gal4>Yap* eye discs (fig. 4A and supplementary fig. S6A–E, Supplementary Material online). We first determined the endogenous targets of *GMR-Gal4*-driven *Drosophila* Yki and then utilized the highly active *Trichoplax Yap* and *Monosiga Yap* containing the human TBD (Yap<sup>+TBD</sup>) to define core target genes activated in common. In addition, we used *Monosiga Yap*, which was not able to induce ectopic proliferation, as a negative control to remove the transcriptional background resulting from protein overexpression. For each of these conditions, the transcriptional profile was compared with that of a *GMR-Gal4>UAS-GFP* control.

RNA-seq analysis identified a robust gene expression signature common to eumetazoan Yaps as well as the form of *Monosiga Yap<sup>+TBD</sup>* (fig. 4B; supplementary table S1, Supplementary Material online). Validating our approach, this signature comprised 213 commonly upregulated targets that included almost all previously known Yki target genes (*cyclin E* [Tapon et al. 2002], *expanded* [Hamaratoglu et al. 2006], *e2f1* [Goulev et al. 2008], *wingless* [Cho et al. 2006], *dally* [Baena-Lopez et al. 2008], *kibra* [Genevet et al. 2010], and *vein* [Zhang, Ji, et al. 2009]), along with 258 commonly downregulated factors (fig. 4B). Interestingly, most of these genes were conserved in the *Trichoplax* and *Monosiga* genomes (supplementary table S2, Supplementary Material online), perhaps representing an ancient Yap-dependent gene expression signature. Among the 213 commonly upregulated targets, 16 genes were subsequently validated by real-time quantitative PCR analysis (supplementary fig. S7, Supplementary Material online). Although we observed a highly significant overlap between eumetazoan Yap target genes in *Drosophila*, only 4% and 11% of these genes were correspondingly up- and downregulated by *Monosiga Yap*, respectively (fig. 4B). This

FIG. 3. Continued

Scale bar = 50  $\mu$ m. (C–C') *diap1-lacZ* expression (red) in eye discs overexpressing the corresponding Yap orthologs in clones (GFP+, green) and stained with Hoechst (blue). Except for *AqYap<sup>S95A</sup>* and *MbYap<sup>S48A</sup>*, elevated *diap1-lacZ* expression was detected in all Yap ortholog-overexpressing clones (yellow arrowheads). Scale bar = 50  $\mu$ m. (D) Pupal retinæ from the genotypes indicated above, stained with anti-Armadillo antibody to visualize cell outlines at 42 h after puparium formation. Scale bar = 10  $\mu$ m. (E) Corresponding scanning electron micrographs (SEM) of adult retinæ. (F) Quantification of IOCs per ommatidia in controls (*w*, *GMR-Gal4/+*; *n* = 20) and following expression of *Amphimedon Yap* (*GMR-Gal4>AqYap<sup>S95A</sup>*; *n* = 20). Statistical analysis was performed using Student's *t*-test (\**P* < 0.001). (G, H) Edu incorporation assay in eye discs overexpressing chimeric constructs of *Monosiga Yap* (G) and *Amphimedon Yap* (H) with the *Homo* TBD. Addition of the human TBD to either variant resulted in a strong capacity to induce proliferation.

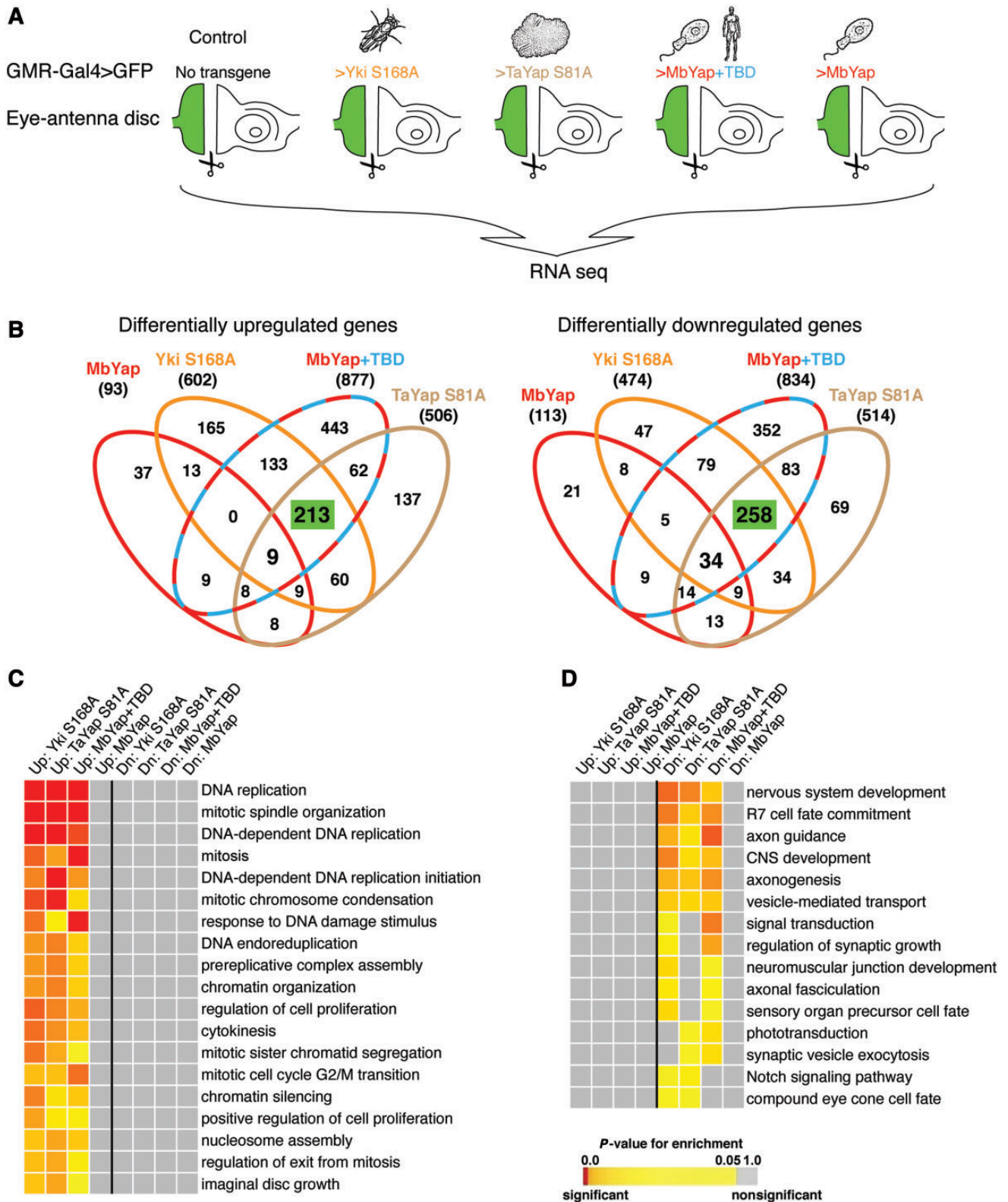


**Fig. 4.** The transcriptional program downstream of Yap ortholog induction. (A) Experimental design for RNA-seq experiment. *Drosophila* Yki (Yki<sup>S168A</sup>), *Trichoplax* Yap (TaYap<sup>S81A</sup>), chimeric *Monosiga* Yap with the human TBD (MbYap<sup>+TBD</sup>), and *Monosiga* Yap (MbYap) were co-overexpressed with UAS-GFP using GMR-Gal4. Control is GMR-Gal4>UAS-GFP. For each experimental condition, total RNA was extracted from surgically dissected GMR expression domains (GFP +). (B) Four-way Venn diagrams of differentially upregulated (left) and downregulated (right) genes in each overexpression condition. The number of genes up- and downregulated is indicated between brackets under each transgene name. The numbers of commonly up- and downregulated genes in Yki<sup>S168A</sup>, TaYap<sup>S81A</sup>, and MbYap<sup>+TBD</sup> are indicated in green boxes. (C, D) Matrices of gene ontology of biological processes analysis for genes upregulated (Up) and downregulated (Dn) in each overexpression condition.

indicates that the transcriptional outputs of Yap with and without the  $\alpha 1$ -loop- $\alpha 2$  TBD are fundamentally distinct. One notable exception was that *expanded (ex)*, a well-defined target of Yki in *Drosophila*, was 1.4-fold upregulated following *Monosiga* Yap expression compared with more than 3-fold induction by metazoan Yap variants (supplementary table S1, Supplementary Material online).

In agreement with the phenotypes induced by Yki/Yap expression (figs. 2A and 3A), GO term analysis indicated that a significant number of commonly upregulated genes were involved in DNA replication, cell cycle, and growth regulation processes (fig. 4C). Interestingly, we found that the average expression level of the top 100 commonly upregulated genes induced by *Trichoplax* Yap and *Monosiga* Yap<sup>+TBD</sup> was higher than that induced by *Drosophila* Yki (supplementary fig. S6F, Supplementary Material online). These quantitative differences in target gene expression level may account for the more extensive cell proliferation induced by these Yap variants (fig. 3A). By contrast to the enrichment of upregulated genes for cell proliferation processes, downregulated genes were enriched for the process of nervous system development (fig. 4D). This is consistent with the observed delays in cell cycle exit and retinal determination/differentiation as a consequence of Yap expression in the eye (fig. 3D and E). Except in the case of *Monosiga* Yap<sup>+TBD</sup>, we did not identify significant Yap ortholog-specific enrichment for biological processes (supplementary fig. S8, Supplementary Material online).

### Genome-Wide Distribution of Yki and Sd on Chromatin

In principle, the Yki/Yap dependent gene expression profiles described above could be the result of primary, secondary, or tertiary transcriptional events. To extend the results of our comparative studies and determine which induced genes were most likely direct targets, we performed a ChIP-Seq experiment to identify the genome-wide occupancy of *Drosophila* Yki in proliferating cells. For chromatin immunoprecipitation, we generated a novel antibody that specifically detects Yki protein (fig. 5A, B-B'', and C-C'') and analyzed dissected eye discs of the genotype *GMR-Gal4>UAS-Yki<sup>S168A</sup>*. In parallel, we performed a ChIP-Seq experiment using Polymerase II (Pol II) antibody as a control. Similar to recent ChIP-Seq analyses of wild-type Yki in wing and eye discs (Oh et al. 2013; Slattery et al. 2013), Yki was enriched with high confidence at a large number of sites throughout the genome (using Model-based Analysis for ChIP-Seq [MACS],  $P < 0.001$ ; supplementary fig. S9, Supplementary Material online). Binding peaks were found in proximity to 5,732 genes (supplementary table S1, Supplementary Material online) and a large number of them were localized within promoter regions (supplementary fig. S10A, Supplementary Material online). To focus our analysis on bona fide targets of the *Drosophila* Yki/Sd complex, we also generated a novel antibody directed against Sd and performed ChIP-seq analysis under the same conditions (fig. 5D, E-E'', and F-F''). The Sd binding peaks were specific because they were highly enriched

for the Sd motif (supplementary fig. S10B, Supplementary Material online). Among the 1,238 genes bound by Sd, 97% were also bound by Yki (supplementary fig. S10C and D, Supplementary Material online), and this high-confidence subset included all previously known target genes (supplementary fig. S11, Supplementary Material online).

To identify novel Yki target genes, we next focused on the overlap between our RNA-seq and ChIP-seq data sets (supplementary fig. S10C and D, Supplementary Material online). We found that Yki and Yki/Sd peaks were highly enriched near upregulated genes (the common set from figure 4B,  $P < 3 \times 10^{-16}$ ; Fisher test) but not near downregulated genes ( $P = 0.3$  for Yki and  $P = 0.08$  for Yki/Sd). Interestingly, the genes induced in common by different Yap orthologs showed a higher enrichment of Yki and Yki/Sd peaks (78% and 32%, respectively) compared with the analysis of solely Yki-induced genes (64% for Yki peaks and 24% for Yki/Sd peaks). These results corroborate the predominant function of Yki/Yap as a transcriptional activator and led us to the identification of several novel putative targets. Most prominently, the Hippo pathway components *warts (wts)*, *fat (ft)*, and *dachsous (ds)* were commonly upregulated targets and exhibited both Yki and Sd peaks, revealing the existence of novel negative feedback loops controlling Yki activity (fig. 6A). Another class of putative direct target genes included the signaling ligands *decapentaplegic (dpp)*, *wnt6*, *spatzle 3 (spz3)*, *vascular endothelial growth factor 2 (pvf2)*, *thrombospondin (tsp)*, *tissue inhibitor of metalloprotease (Timp)*, and *neuropeptide-like precursor 1 (nplp1)* (fig. 6B). Our analysis also highlighted the amino acid transporter *pathetic (path)* and two insulin-signaling components as potential growth-regulatory factors targeted by Yki/Sd activity (*insulin receptor (InR)* and *forkhead box protein O (foxo)*; fig. 6B). In addition to these Yki/Sd target genes, our ChIP-seq data clearly indicate the existence of an Sd-independent downstream program that is most likely the result of Yki's putative interactions with other DNA-binding partners, such as Homothorax, Teashirt, and Mad (Peng et al. 2009; Oh and Irvine 2011). Indeed, using a recent ChIP-Seq analysis of Homothorax in eye discs (Slattery et al. 2013), we found that 40% of these Sd-independent targets were cobound by Yki and Homothorax (supplementary table S3, Supplementary Material online). Together, these findings reveal a complex network of factors downstream of Yap activation and directly link Hippo signaling to the regulatory architecture for a wide variety of processes required for tissue growth in vivo.

### A Yap/Yki-Induced Transcriptional Program Shared by *Drosophila* and Vertebrates

In vertebrates, Yap-induced genes have been identified by microarray profiling of hepatocytes, fibroblasts, and breast epithelial cells (Overholtzer et al. 2006; Dong et al. 2007; Hao et al. 2008; Lu et al. 2010). To interpret our transcriptional profiling results at an evolutionary level and investigate the extent to which Yap's transcriptional output is conserved, we took advantage of the OrthoDB catalog of eukaryotic orthologs (Waterhouse et al. 2011) to test for orthologous

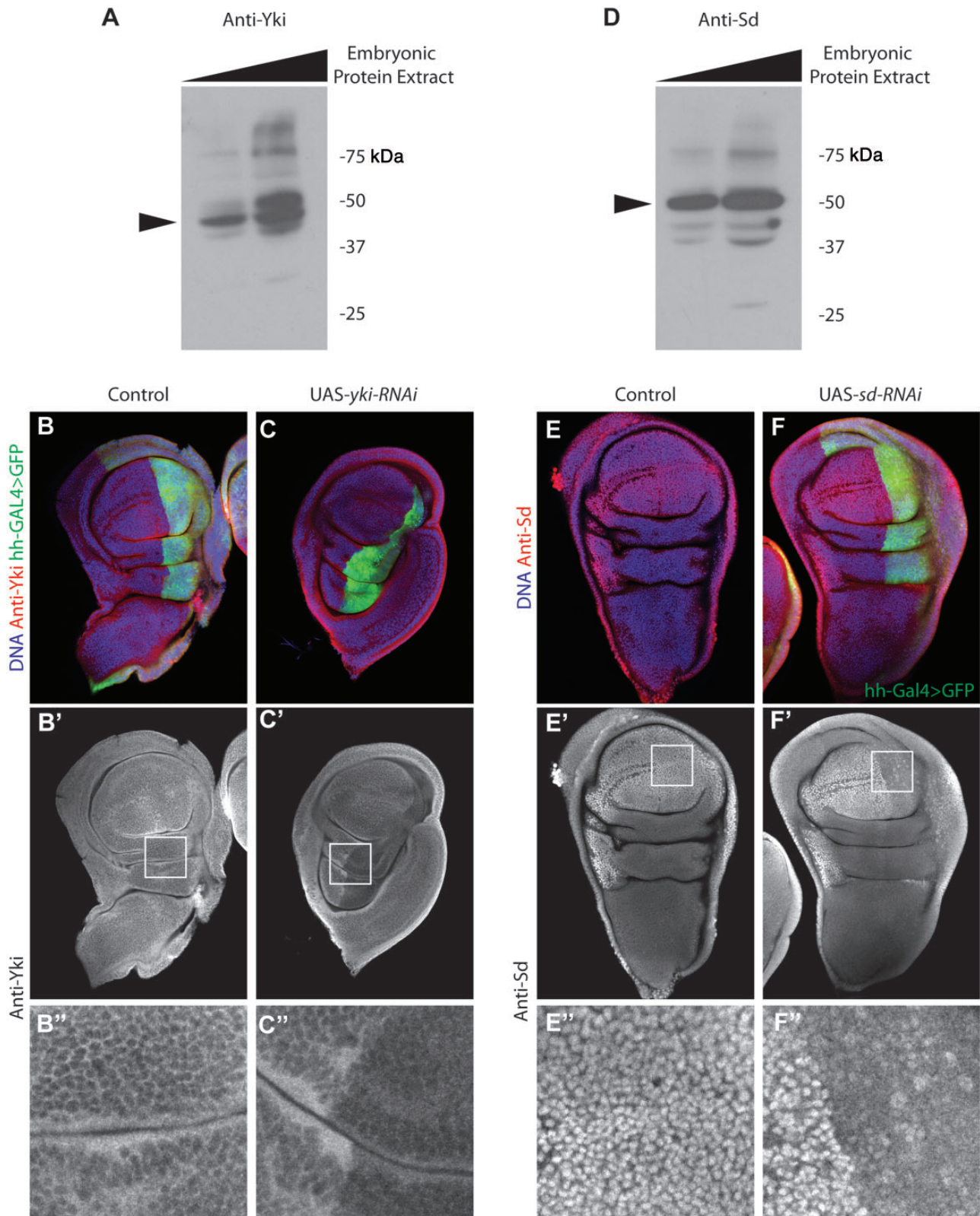


**Fig. 5.** Validation of anti-Yki and anti-Sd antibodies. (A) Western blot analysis shows that anti-Yki antibody detects a strong signal at the expected molecular weight (arrowhead, 45 kDa). (B–B'') Control wing disc stained with Hoechst (blue) and anti-Yki (red). The posterior compartment is marked by the expression of *hh-Gal4>UAS-GFP* (green). Anti-Yki detects ubiquitous expression of Yki. (C–C'') Wing disc overexpressing *UAS-yki-RNAi* under the control of *hh-Gal4*. The clear reduction of anti-Yki staining in the posterior compartment (inset box) confirms that our antibody recognizes *Drosophila* Yki. (D) Anti-Sd detects a specific band at the expected molecular weight (arrowhead, 50 kDa). (E–E'') Control wing disc stained with Hoechst (blue) and anti-Sd (red). Endogenous *sd* expression is elevated in the wing pouch and margin, which is consistent with our Anti-Sd staining. (F–F'') A wing disc expressing *UAS-sd-RNAi* under the control of *hh-Gal4* shows a strong reduction of Sd staining in the posterior compartment (inset box), confirming the specificity of Anti-Sd.

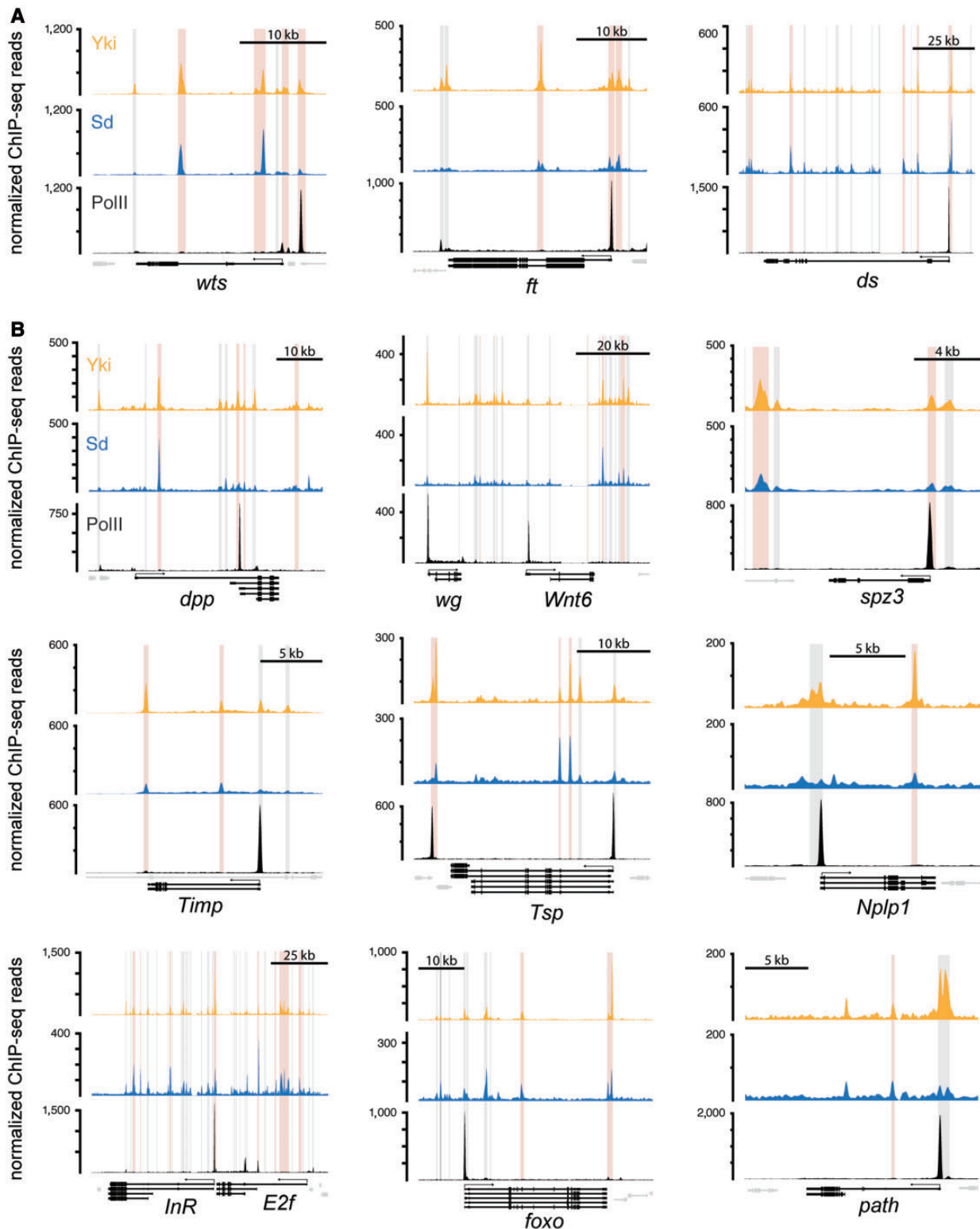


**FIG. 6.** Chromatin localization of Yki and Sd on novel target genes. Plots of Yki (orange), Sd (blue), and PolII (black) occupancy peaks in selected commonly upregulated genes from the RNA-seq data. (A) Target genes belonging to novel negative feedback loops. (B) Novel target genes. Transcriptional units of target genes are highlighted in black and their neighbor genes are in gray. Pink and gray bars indicate significant Yki/Sd and Yki peaks, respectively.

relationships between genes induced by Yap in mouse liver (Dong et al. 2007) and those in our *Drosophila* RNA-seq data. Strikingly, despite the cell type differences and the substantial evolutionary distance between these two organisms, 74

Yap-induced genes from the mouse experiments were also significantly upregulated in *Drosophila* (supplementary table S4, Supplementary Material online). At least 63 and 31 of these 74 genes show Yki/Yap binding in *Drosophila* and

mouse, respectively (supplementary table S4, Supplementary Material online; [Lian et al. 2010]). Although most of these bilaterian Yap targets belonged to the core DNA replication and cell cycle machinery, we noted the following key conserved targets: *dpp/Bmp4*, *dally/Gpc3*, *wts/Lats2*, *fat/Fat4*, *foxo/Foxo3a*, and *Timp/Timp2*. Consistent with this, *Bmp4* was recently validated as a key transcriptional target of the Hippo pathway in mammary cells (Lai and Yang 2013). However, only 28 of these 74 common genes were upregulated following Warts loss of function in *Drosophila*, and only 18 were induced following Mst1-2 loss of function in mouse (supplementary table S4, Supplementary Material online; [Oh et al. 2013; Lu et al. 2010]). While allowing for substantial context-specific transcriptional effects, our results show the potential utility of comparative methodologies and hint at the existence of an ancient growth-promoting gene expression profile downstream of Yap throughout Bilateria.

## Discussion

In a search for the origins of animal complexity, comparative genomic and evolutionary analyses have generated a wealth of knowledge about the potential genetic toolkit of the metazoan common ancestor (King 2004; Putnam et al. 2007; King et al. 2008; Srivastava et al. 2008, 2010). Generally, these studies emphasize the evolution of molecules that direct cell–cell adhesion, cell differentiation, and body axis formation (Nichols et al. 2006; Abedin and King 2008; Larroux et al. 2008; Richards et al. 2008; Sebe-Pedros et al. 2010; Holstein et al. 2011). Here, we contribute a new perspective: that the development and diversification of complex animal body plans must have also required the incorporation of new mechanisms to coordinately control the patterns of cell growth, proliferation, and survival in a multicellular context. We substantiate this view with a detailed functional analysis of the evolution of a critical growth regulator, the Hippo pathway effector Yap, a transcriptional coactivator whose activity is mediated by its evolutionary conserved DNA-binding partner TEAD.

Using *Drosophila* as a uniform in vivo experimental system, we compared the activity of representative Yap orthologs from major animal lineages and their closest unicellular relatives, thus providing insight into the evolutionary history of Yap protein structure and function throughout 700 My of evolution. Although directed studies will be required to test the taxon-specific requirements for Yap in Metazoa and its closest unicellular relatives, our results nevertheless provide clear experimental support for the ubiquity of the Yap-TEAD complex as a key functional unit that possesses growth-promoting activity. Importantly, the variable effects of different Yap orthologs in *Drosophila* could be attributed to numerous structural differences that could enhance or reduce their activity or regulation.

As evidence for coevolution of the Yap-TEAD complex, we report that the eumetazoan interaction interfaces are distinct from those in the premetazoan and sponge complexes (fig. 1C). This suggests strong evolutionary constraints and highlights the importance of these transcriptional cofactors as a building block for the evolution of animal growth control.

Our results also define the Yap-TEAD interaction as a new model system for understanding the coevolution of protein complexes during the emergence of animal multicellularity. Interestingly, a similar evolutionary scenario was recently described for another central growth regulator, the Myc-Max complex. However, cross-species interactions between *Monosiga* and human Myc and Max were not detected (Young et al. 2011). Thus, we propose that the structural changes in these protein complexes (Yap-TEAD and Myc-Max) may have served as critical adaptations for multicellular growth control during their co-option into an ancient metazoan gene regulatory architecture.

The presence of the most critical Warts/Lats phosphorylation site in all Yap orthologs (fig. 1B) suggests the conservation of Lats-Yap phosphoregulation. Consistent with this, we observed an enhancement of Yap activity following the modification of this critical site in the metazoan forms of Yap (fig. 2A and B). In addition, it has been reported that the activity of *Capsaspora* Yap is regulated through phosphorylation, pushing back the origin of Lats-Yap phosphoregulation to the unicellular ancestors of animals (Sebe-Pedros et al. 2012). Because it is thought that the modern Hippo/Lats pathway responds to extracellular cues to regulate tissue growth, it remains unclear what function this pathway may have served in a hypothetical unicellular ancestor of animals. One possibility is that the pathway regulated growth in multicellular aggregates or in response to local density of specific cell types. Analyses that examine the downstream transcriptional output of Yap TEAD signaling in close metazoan relatives could shed light on this important issue.

Beyond the evolutionary implications of these results, our functional phylogenomic approach also provided mechanistic insights into the contemporary Hippo pathway itself. Although recent studies have analyzed the genome-wide occupancy of Yki during normal development (Oh et al. 2013; Slattery et al. 2013), here we used a combination of RNA-seq and ChIP-seq experiments to identify novel Yki and Sd target genes induced during cell proliferation. Indeed, we report the existence of a core gene expression signature underlying the control of tissue growth in *Drosophila* (fig. 4B and supplementary table S1, Supplementary Material online). This signature includes novel target genes that could mediate cross talk with key signaling pathways, as well as multiple feedback loops controlling Yap activity (fig. 7). Further experimental analyses would be required to know when and where Yki regulates these novel targets during normal development.

On a broader note, although it is widely accepted that the incredible diversity of animal development is directed by a limited number of conserved signaling pathways (Pires-daSilva and Sommer 2003), it remains unclear whether these pathways act, at least partially, through conserved downstream genetic programs. By comparing the transcriptional output of Yap in *Drosophila* and mouse, we identified a conserved set of target genes commonly induced in these evolutionarily distant species (supplementary table S4, Supplementary Material online). These targets may represent an ancestral gene-expression signature of Yap and constitute candidate effectors of Yap-TEAD activity in other metazoans.

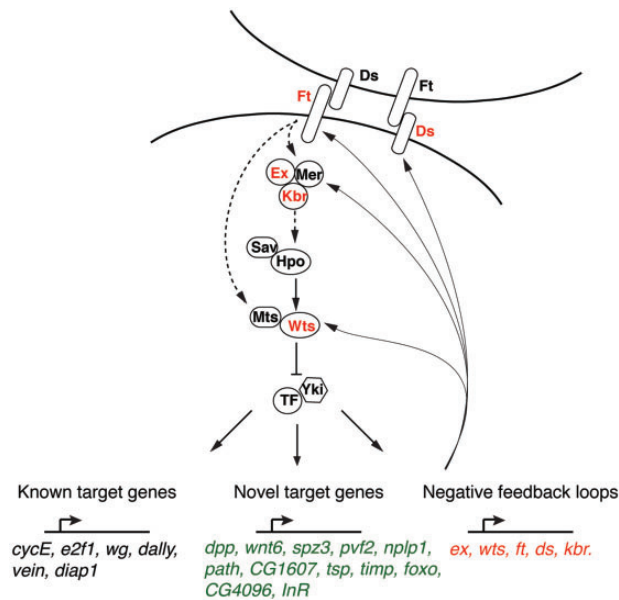


**Fig. 7.** Novel downstream target genes of Yki in *Drosophila*. Schematic representation of the Fat-Hippo pathway in *Drosophila*. In response to dachsous (Ds) binding, fat (Ft) protocadherin activates the Hippo pathway, potentially through expanded and warts (dashed line). The Expanded-Merlin-Kibra complex (Ex-Mer-Kbr) also activates the kinase cascade leading from the Hippo/Warts (Hpo/Wts) kinases and their scaffolding proteins Salvador (Sav) and Mod as tumor suppressor (Mts) to Yki and its transcriptional cofactors (TF). Listed below are examples of putative target genes that met the dual criteria of Yki/Sd chromatin association and were upregulated in common following *Yki*<sup>S168A</sup>, *TaYap*<sup>S81A</sup>, and *MbYap*<sup>+TBD</sup> overexpression. Yap ortholog-induced genes were divided into three classes: known target genes, novel target genes (green), and candidate negative feedback loop components (red).

Additional analyses would be required to characterize these potentially conserved targets in depth. Combined, these results illustrate the power of comparative studies to provide both evolutionary and mechanistic insight into fundamental biological processes.

## Materials and Methods

### Bioinformatics

We identified Yap genes using the basic alignment sequence tool (Blast: TblastN, TblastX, and BlastP) with human Yap as a query. The genomes of *N. vectensis*, *T. adhaerens*, *A. Queenslandica*, and *M. brevicollis* are available in <http://genome.jgi-psf.org/Nemve1>, <http://genome.jgi-psf.org/Triad1> (last accessed February 23, 2014) (spongezome.metazome.net), and <http://genome.jgi-psf.org/Monbr1> (last accessed February 23, 2014). *Capsaspora owczarzaki* and *S. rosetta* genome assemblies were examined on the Broad Institute web site (<http://www.broadinstitute.org/>, last accessed February 23, 2014). Reciprocal best Blast searches and protein domain structure analyses (Pfam: <http://pfam.sanger.ac.uk/search> [last accessed February 23, 2014] and SMART: <http://smart.embl-heidelberg.de> [last accessed February 23, 2014]) were used to screen for positive hits. To identify the TBD, we conducted a protein structure homology analysis using

the SWISS-MODEL automated comparative protein-modeling server (<http://swissmodel.expasy.org>, last accessed February 23, 2014). Yap orthologs were aligned using MUSCLE (Edgar 2004) with default settings. For phylogenetic analyses, the alignment was manually curated to only retain the two well-conserved WW domains. Neighbor-joining trees were generated using Phylip with default settings and 10,000 bootstrap replicates. Maximum likelihood analyses were run with 1,000 bootstrap replicates using PhyML with the Whelan and Goldman (WAG) model of amino acid substitution, four substitution rate categories, and the proportion of invariable sites estimated from the data set. Bayesian inference methods were implemented using MrBayes v3.1.2 with a mixed amino acid model prior and a variable rate prior.

### Cloning

The full-length coding sequence of *Nematostella* Yap was amplified from larval cDNA using the following primers: *Nematostella*-YapF: 5'-TTC ACA ATG GAA AGG AAA AAC A-3'; *Nematostella*-YapR: 5'-TCG GAC TAC AAC CAA GTT AAA AA-3'. The amplified cDNA was cloned into the pCRTM4-TOPO vector (Invitrogen). The coding sequences of Yap from *Monosiga*, *Amphimedon*, *Trichoplax*, *Drosophila*, and *Human* were synthesized by GenScript (Piscataway, NJ). *Amphimedon* Yap was also cloned from larval cDNA into the pCRTM4-TOPO vector using the following primers: *Amphimedon*-YapF: 5'-ATG ACT GAT ATT ATC AAT ACG AAT TCC CCT TCC-3'; *Amphimedon*-YapR: 5'-CAC CCA AGT ATT ACT ACC AAA CAT TCC-3'. To generate the hypothetically nonphosphorylatable form of each protein, serine to alanine mutations were introduced by primer-mediated site-directed mutagenesis. Chimeric constructs of *Monosiga* Yap and *Amphimedon* Yap with the human TBD were synthesized by GenScript. All GenScript constructs were cloned into the pUC57 plasmid EcoRV site.

For phiC31-mediated site-specific transformation, all constructs were cloned into the *pUAST-attB* vector using BglII-NotI or NotI-XbaI sites. *Nematostella* warts (*Nvwarts*) was amplified from larval cDNA and cloned into the pCRTM4-TOPO vector using the following primers: *Nematostella* wartF: 5'-TGG CCC TCA ACA TAC CAA GGA GTA AG-3'; *Nematostella* wartR: 5'-AAG AAT GCA TGT TCT GGA CGA TGG TT-3'. We then cloned *Nvwarts* into NotI-digested *pCaSpeR-hs*.

### Protein Stability of Yap/Yki Orthologs

To generate C-terminal human influenza hemagglutinin (HA) fusion proteins of Yap orthologs, the coding sequences of each protein were cloned in frame with the HA coding sequences in *pHWH* (*Drosophila* Genomics Resource Center) using Gateway cloning (Invitrogen). Yap-HA constructs were transfected into *Drosophila* S2 cells using Effectene Transfection Reagent Kit (Qiagen) following the manufacturer's instructions. Transfected S2 cells were incubated for 24 h and heat shocked for 1 h to induce Yap-HA expression. Cell lysates were collected 3, 6, and 12 h postheat shock and analyzed by Western blotting with Anti-HA (Sigma-Aldrich,

1:4,000) and anti- $\alpha$ -tubulin (Sigma-Aldrich, 1:500) as a loading control.

### Coimmunoprecipitation

We generated N-terminal HA and C-terminal Flag fusion proteins of TEAD and Yap, respectively. The full coding sequences of TEAD/Sd from *Amphimedon*, *Nematostella*, and *Drosophila* were amplified from their corresponding adult cDNAs and cloned in frame with the HA coding sequences in *pAHW* (*Drosophila* Genomics Resource Center) using the Gibson assembly kit (NEB). Using the same approach, we also cloned the coding sequences of the phosphomutant forms of Yap/Yki in frame with the coding sequence of Flag in *pAWF* (*Drosophila* Genomics Resource Center). *Drosophila* S2 cells were transiently transfected with these constructs as indicated above. After 3 days, cells were lysed (lysate buffer: 50 mM Tris pH7.4, 150 mM NaCl, 5 mM MgCl<sub>2</sub>, 5% glycerol, 0.5% Triton X-100, and 1× protease inhibitor cocktail [Roche]) and centrifuged at 16,000 × g for 10 min. Coimmunoprecipitations were performed using Dynabeads Protein G immunoprecipitation kit (Life Technologies) following the manufacturer's instructions.

### *Drosophila* Stocks

All transgenic flies carrying *UAS-attB* transgenes were created by phiC31-mediated site-specific transformation using the attP2 site (Groth et al. 2004; Bischof et al. 2007). These transgenes were overexpressed using either *GMR-Gal4* or *GMR-Gal4* with *UAS-EGFP*. The expression of *diap1* was monitored using *th<sup>15c8</sup> (diap1-lacZ)* (Hay et al. 1995). To test the specificity of anti-Yki and anti-Sd antibodies in vivo, *UAS-yki-RNAi* (Bloomington, 34067) and *UAS-sd-RNAi* (Bloomington, 35481) were overexpressed using *hh-Gal4*. For the *Drosophila warts* rescue experiment, we crossed *yw, eyeless-FLP; FRT82B/TM6 Tb* (Bloomington, 5620) to *w, hs-Nvwarts/hs-Nvwarts; wts<sup>X1</sup> FRT82B/TM6 Sb Tb*. Expression of *hs-Nvwarts* was induced by heat shock for 1 h every day from the second instar larval stage until eclosion. *wts<sup>X1</sup>* is described in Xu et al. (1995).

### Eye Width Measurement

For measuring adult eyes, flies were decapitated using a sharp razor blade. The heads were imaged using a Leica MZ 16F microscope. To determine eye width, two parallel lines were drawn at the edges of each eye. The distance separating these two lines was measured using ImageJ.

### Edu Incorporation

EdU incorporation was detected using the Click-iT Alexa Fluor 488 imaging kit (Invitrogen). Third instar eye imaginal discs were incubated for 30 min with 300  $\mu$ M EdU in Ringer's solution. After fixation, samples were stored for at least 1 h in 100% methanol at  $-20^{\circ}$ C. All subsequent steps were conducted according to the manufacturer's protocol.

### Generation of Yki and Sd antibodies

Custom-made polyclonal rabbit anti-Yki and anti-Sd antibodies were generated and affinity purified by GenScript. They were raised against the N-terminal 243 amino acids of Yki and the full-length protein of Sd. For Western blots, anti-Yki and Anti-Sd dilutions were 1:2,000 and 1:4,000, respectively.

### Immunocytochemistry

Imaginal discs and pupal retina were fixed and processed according to standard protocols. Primary antibodies used were anti-Cyclin E (Santa Cruz Biotechnology, 1:500), anti- $\beta$ -galactosidase (Sigma-Aldrich, 1:1,000), anti-Armadillo (Developmental Studies Hybridoma Bank, 1:400), anti-Yki (1:1,000), and anti-Sd (1:1,000).

### RNA Extraction, Library Preparation, Sequencing, and RNA-Seq Analysis

Total RNA was recovered from surgically isolated GMR expression domains (GFP+) from 25 to 30 third instar eye discs using a RNeasy kit (Qiagen). For each genotype, total RNA extraction was conducted in triplicate. Total RNA (400 ng) was enriched for poly(A) + RNA by oligo(dT) selection. The Poly(A) + RNA was then fragmented, and first-strand cDNA synthesis was performed using random hexamer priming in the Stowers Institute Molecular Biology Core facility, where all subsequent steps were conducted. Following second-strand synthesis, the ends were cleaned up, a nontemplated 3' adenosine was added, and Illumina indexed adapters were ligated to the ends. The libraries were enriched by 15 rounds of polymerase chain reaction (PCR). The purified libraries were quantified with the high-sensitivity DNA assay on an Agilent 2100 Bioanalyzer. Equal molarities of individual libraries were pooled together (five libraries per pool) for multiplex sequencing. Pooled libraries were sent to Tufts (TUCF) for single read sequencing (50 nt) on a HiSeq 2000, and fastq files were returned.

For analysis, sequence reads in fastq format were mapped to the *Drosophila* genome using tophat-1.0.14 (Trapnell et al. 2009) against Flybase 5.29 (dm3 compatible). Flybase transcripts (v5.29) were quantified and compared between control and each overexpression condition using cuffdiff-1.0.2 (Trapnell et al. 2010). Genes with adjusted *P* values of less than 0.05 were selected for functional annotation based on Gene Ontology (GO Consortium 2006). Enrichment analysis was performed using Gtools (<http://www.gitools.org>, last accessed February 23, 2014) to identify biological processes that were enriched among up- or downregulated genes.

### Quantitative Real-Time PCR

To independently validate the RNA-seq results, total RNA was isolated as described above. Five independent RNA extractions were performed for each genotype. Following cDNA generation, each real-time quantitative PCR (qPCR) reaction contained 0.33 ng of cDNA and a PCR master mix including 0.5  $\mu$ M of each primer and 1× PerfeCTa SYBR Green FastMix from Quanta Biosciences (cat. no. 95072-250) in 10  $\mu$ l total reaction using a CAS-4200 qPCR loading robot from Corbett

Life Science. qPCR reactions were performed in 384-well format on a 7900HT Real-Time PCR Detection System from Applied Biosystems. Results were analyzed using qBase Plus software from Biogazelle. *actin*, *GAPDH*, and *tbp* genes were used as endogenous controls and the calibrated normalized relative quantity (CNRQ) values were calculated for each tested gene. Primers are available on request.

### ChIP-Seq

Chromatin immunoprecipitation from eye discs was performed using a modified protocol from Gaertner et al. (2012). First, third instar larvae were dissected in phosphate buffered saline (PBS) (pH 7.4) such that only eye discs and brain remained attached to the mouth hooks. The dissected material was subsequently fixed in 1 ml fixation buffer (50 mM 4-(2-hydroxyethyl)-1-piperazineethanesulfonic acid [HEPES], pH 7.5; 1 mM ethylenediaminetetraacetic acid [EDTA]; 0.5 mM ethylene glycol tetraacetic acid [EGTA]; 100 mM NaCl; 2% formaldehyde) for 30 min at room temperature. After four washes (PBS, pH 7.4; 0.1% Triton X-100; 0.1% Tween-20), eye discs were hand-dissected and combined into pools of 200 discs in 300  $\mu$ l buffer A2 (15 mM HEPES, pH 7.5; 140 mM NaCl; 1 mM EDTA; 0.5 mM EGTA; 1% Triton X-100; 0.1% sodium deoxycholate; 0.1 % sodium dodecyl sulfate [SDS]; 0.5 % *N*-lauroylsarcosine; 1 $\times$  Roche complete protease inhibitor cocktail, cat. no. 5056489001). Sonication was performed in a Bioruptor sonicator for 30 min (30 s on/off cycle at the “high” setting). Following centrifugation (16,000  $\times$  g; 10 min at 4  $^{\circ}$ C), the supernatant containing soluble chromatin was transferred to fresh tubes, and 50  $\mu$ l was set aside as whole cell extract (WCE; input).

Per ChIP, 10  $\mu$ g antibodies were added to 450  $\mu$ l chromatin (corresponding to approximately 300 discs) and incubated overnight at 4  $^{\circ}$ C with rotation. We used the following antibodies: anti-Pol II (Covance 8WG16, cat. no. MMS-126R; mouse monoclonal antibody), anti-Sd, and anti-Yki. Immunocomplexes were purified by adding 50  $\mu$ l prewashed Dynabeads coated with protein A/protein G (Life Technologies, cat. no. 10002D and 10004D) for 4 h, rotating at 4  $^{\circ}$ C. The beads were washed three times in radioimmunoprecipitation assay buffer (RIPA) buffer (50 mM HEPES, pH 7.5; 1 mM EDTA; 0.7% sodium deoxycholate; 1% NP-40; 500 mM LiCl) and once in TE. Immunoprecipitated DNA was eluted twice in 75  $\mu$ l elution buffer (50 mM Tris, pH 8.0; 10 mM EDTA; 1% SDS) at 65  $^{\circ}$ C to maximize yields. Crosslinks of ChIP and WCE DNA were reversed overnight at 65  $^{\circ}$ C. DNA was purified by RNase A (Sigma, cat. no. R6513; [0.2  $\mu$ g/ $\mu$ l]; 1 h at 37  $^{\circ}$ C) and proteinase K (Life Technologies, cat. no. AM2546; [0.2  $\mu$ g/ $\mu$ l]; 2 h at 55  $^{\circ}$ C) treatment followed by phenol/phenol–chloroform–isoamylalcohol extractions and ethanol precipitation. The precipitated DNA was resuspended in 30  $\mu$ l 10 mM Tris buffer (pH 8).

For ChIP-seq library preparation, 30  $\mu$ l ChIP DNA and 100 ng WCE DNA were used to construct ChIP-Seq libraries with the NEBNext ChIP-seq Library Prep Master Mix Set (cat. no. E6200L) and the NEBNext Multiplex Oligos (cat. no. E7335S and E7500S) for Illumina, following the manufacturer’s

instructions. Concentration and size distribution of the libraries were assessed on an Agilent 2100 Bioanalyzer (high-sensitivity DNA assay chip). Sequencing was performed on an Illumina HiSeq2500 instrument, with 50 bp single reads in the high-output mode.

All sequence reads were filtered to include only those passing the standard Illumina quality filter and then aligned to the *Drosophila melanogaster* reference genome (UCSC dm3 release) using Bowtie version 0.12.9, with the following parameters: -v 2 -k 1 -m 3 -best -strata. Peaks were called with MACS v2.0.10.20120913 (Zhang, Liu, et al. 2008), using an adjusted *P* value of 0.001 and 0.01 for Yki and Sd, respectively. To assign a peak to its nearest gene, the following criteria were used: If the peak overlapped a gene, it was assigned to that gene regardless of where the overlap occurred; otherwise, it was assigned to the gene if the peak summit occurred within 1,500 bp upstream of the transcription start site.

ChIP-seq and RNA-seq data are available under Gene Expression Omnibus (GEO) accession number GSE54603.

### Supplementary Material

Supplementary figures S1–S11 and tables S1–S4 are available at *Molecular Biology and Evolution* online (<http://www.mbe.oxfordjournals.org/>).

### Acknowledgments

The authors thank B. Degnan, L. Grice, C. Conaco and K. Kosik for providing the *Amphimedon* cDNA; A. Peak and K. Zueckert-Gaudenz for RNA-seq library preparation and sequencing; K. Walton and A. Perera for ChIP-seq library sequencing; B. Fleharty and W. McDowell for real-time quantitative PCR analysis; J. Johnston for assistance with bioinformatic analysis; T. Akiyama for his suggestions on the co-immunoprecipitation experiments; and L. Gutchewsky for administrative support. Financial support was provided by the Stowers Institute for Medical Research and from a Burroughs Wellcome Fund Career Award in Biomedical Sciences to M.C.G.

### References

- Abedin M, King N. 2008. The premetazoan ancestry of cadherins. *Science* 319:946–948.
- Baena-Lopez LA, Rodriguez I, Baonza A. 2008. The tumor suppressor genes *dachsous* and *fat* modulate different signalling pathways by regulating dally and dally-like. *Proc Natl Acad Sci U S A*. 105: 9645–9650.
- Bischof J, Maeda RK, Hediger M, Karch F, Basler K. 2007. An optimized transgenesis system for *Drosophila* using germ-line-specific phiC31 integrases. *Proc Natl Acad Sci U S A*. 104:3312–3317.
- Camargo FD, Gokhale S, Johnnidis JB, Fu D, Bell GW, Jaenisch R, Brummelkamp TR. 2007. YAP1 increases organ size and expands undifferentiated progenitor cells. *Curr Biol*. 17:2054–2060.
- Chen L, Chan SW, Zhang X, Walsh M, Lim CJ, Hong W, Song H. 2010. Structural basis of YAP recognition by TEAD4 in the Hippo pathway. *Genes Dev*. 24:290–300.
- Cho E, Feng Y, Rauskolb C, Maitra S, Fehon R, Irvine KD. 2006. Delineation of a fat tumor suppressor pathway. *Nat Genet*. 38: 1142–1150.

- Dong J, Feldmann G, Huang J, Wu S, Zhang N, Comerford SA, Gayyed MF, Anders RA, Maitra A, Pan D. 2007. Elucidation of a universal size-control mechanism in *Drosophila* and mammals. *Cell* 130: 1120–1133.
- Edgar RC. 2004. MUSCLE: a multiple sequence alignment method with reduced time and space complexity. *BMC Bioinformatics* 5:113.
- Gaertner B, Johnston J, Chen K, Wallaschek N, Paulson A, Garruss AS, Gaudenz K, de Kumar B, Krumlauf R, Zeitlinger J. 2012. Poised RNA polymerase II changes over developmental time and prepares genes for future expression. *Cell Rep.* 2:1670–1683.
- Gene Ontology C. 2006. The Gene Ontology (GO) project in 2006. *Nucleic Acids Res.* 34:D322–6.
- Genevet A, Wehr MC, Brain R, Thompson BJ, Tapon N. 2010. Kibra is a regulator of the Salvador/Warts/Hippo signaling network. *Dev Cell.* 18:300–308.
- Goulev Y, Fauny JD, Gonzalez-Marti B, Flagiello D, Silber J, Zider A. 2008. SCALLOPED interacts with YORKIE, the nuclear effector of the Hippo tumor-suppressor pathway in *Drosophila*. *Curr Biol.* 18: 435–441.
- Groth AC, Fish M, Nusse R, Calos MP. 2004. Construction of transgenic *Drosophila* by using the site-specific integrase from phage phiC31. *Genetics* 166:1775–1782.
- Hamaratoglu F, Willecke M, Kango-Singh M, Nolo R, Hyun E, Tao C, Jafar-Nejad H, Halder G. 2006. The tumour-suppressor genes *NF2/Merlin* and *expanded* act through Hippo signalling to regulate cell proliferation and apoptosis. *Nat Cell Biol.* 8:27–36.
- Hao Y, Chun A, Cheung K, Rashidi B, Yang X. 2008. Tumor suppressor LATS1 is a negative regulator of oncogene YAP. *J Biol Chem.* 283: 5496–5509.
- Hay BA, Wassarman DA, Rubin GM. 1995. *Drosophila* homologs of baculovirus inhibitor of apoptosis proteins function to block cell death. *Cell* 83:1253–1262.
- Hilman D, Gat U. 2011. The evolutionary history of YAP and the hippo/YAP pathway. *Mol Biol Evol.* 28:2403–2417.
- Holstein TW, Watanabe H, Ozbek S. 2011. Signaling pathways and axis formation in the lower metazoa. *Curr Topics Dev Biol.* 97: 137–177.
- Huang J, Wu S, Barrera J, Matthews K, Pan D. 2005. The Hippo signaling pathway coordinately regulates cell proliferation and apoptosis by inactivating Yorkie, the *Drosophila* homolog of YAP. *Cell* 122: 421–434.
- King N. 2004. The unicellular ancestry of animal development. *Dev Cell.* 7:313–325.
- King N, Hittinger CT, Carroll SB. 2003. Evolution of key cell signaling and adhesion protein families predates animal origins. *Science* 301: 361–363.
- King N, Westbrook MJ, Young SL, Kuo A, Abedin M, Chapman J, Fairclough S, Hellsten U, Isogai Y, Letunic I, et al. 2008. The genome of the choanoflagellate *Monosiga brevicollis* and the origin of metazoans. *Nature* 451:783–788.
- Lai D, Yang X. August 2013. BMP4 is a novel transcriptional target and mediator of mammary cell migration downstream of the Hippo pathway component TAZ. *Cell Signal.* 25(8):1720–1728.
- Larroux C, Luke GN, Koopman P, Rokhsar DS, Shimeld SM, Degnan BM. 2008. Genesis and expansion of metazoan transcription factor gene classes. *Mol Biol Evol.* 25:980–996.
- Li Z, Zhao B, Wang P, Chen F, Dong Z, Yang H, Guan KL, Xu Y. 2010. Structural insights into the YAP and TEAD complex. *Genes Dev.* 24: 235–240.
- Lian I, Kim J, Okazawa H, Zhao J, Zhao B, Yu J, Chinnaiyan A, Israel MA, Goldstein LS, Abujarour R, et al. 2010. The role of YAP transcription coactivator in regulating stem cell self-renewal and differentiation. *Genes Dev.* 24:1106–1118.
- Liu H, Jiang D, Chi F, Zhao B. 2012. The Hippo pathway regulates stem cell proliferation, self-renewal, and differentiation. *Protein Cell* 3: 291–304.
- Lu L, Li Y, Kim SM, Bossuyt W, Liu P, Qiu Q, Wang Y, Halder G, Finegold MJ, Lee JS, et al. 2010. Hippo signaling is a potent in vivo growth and tumor suppressor pathway in the mammalian liver. *Proc Natl Acad Sci U S A.* 107:1437–1442.
- Nichols SA, Dirks W, Pearse JS, King N. 2006. Early evolution of animal cell signaling and adhesion genes. *Proc Natl Acad Sci U S A.* 103: 12451–12456.
- Oh H, Irvine KD. 2010. Yorkie: the final destination of Hippo signaling. *Trends Cell Biol.* 20:410–417.
- Oh H, Irvine KD. 2011. Cooperative regulation of growth by Yorkie and Mad through bantam. *Dev Cell.* 20:109–122.
- Oh H, Slattery M, Ma L, Crofts A, White KP, Mann RS, Irvine KD. 2013. Genome-wide association of Yorkie with chromatin and chromatin-remodeling complexes. *Cell Rep.* 3:309–318.
- Overholtzer M, Zhang J, Smolen GA, Muir B, Li W, Sgroi DC, Deng CX, Brugge JS, Haber DA. 2006. Transforming properties of YAP, a candidate oncogene on the chromosome 11q22 amplicon. *Proc Natl Acad Sci U S A.* 103:12405–12410.
- Peng HW, Slattery M, Mann RS. 2009. Transcription factor choice in the Hippo signaling pathway: homothorax and yorkie regulation of the microRNA bantam in the progenitor domain of the *Drosophila* eye imaginal disc. *Genes Dev.* 23:2307–2319.
- Pires-daSilva A, Sommer RJ. 2003. The evolution of signalling pathways in animal development. *Nat Rev Genet.* 4:39–49.
- Putnam NH, Srivastava M, Hellsten U, Dirks B, Chapman J, Salamov A, Terry A, Shapiro H, Lindquist H, Kapitonov VV, et al. 2007. Sea anemone genome reveals ancestral eumetazoan gene repertoire and genomic organization. *Science* 317:86–94.
- Richards GS, Simionato E, Perron M, Adamska M, Vervoort M, Degnan BM. 2008. Sponge genes provide new insight into the evolutionary origin of the neurogenic circuit. *Curr Biol.* 18:1156–1161.
- Sebe-Pedros A, Roger AJ, Lang FB, King N, Ruiz-Trillo I. 2010. Ancient origin of the integrin-mediated adhesion and signaling machinery. *Proc Natl Acad Sci U S A.* 107:10142–10147.
- Sebe-Pedros A, Zheng Y, Ruiz-Trillo I, Pan D. 2012. Premetazoan origin of the Hippo signaling pathway. *Cell Rep.* 1:13–20.
- Slattery M, Voutev R, Ma L, Negre N, White KP, Mann RS. 2013. Divergent transcriptional regulatory logic at the intersection of tissue growth and developmental patterning. *PLoS Genet.* 9: e1003753.
- Srivastava M, Begovic E, Chapman J, Putnam NH, Hellsten U, Kawashima T, Kuo A, Mitros T, Salamov A, Carpenter ML, et al. 2008. The *Trichoplax* genome and the nature of placozoans. *Nature* 454: 955–960.
- Srivastava M, Simakov O, Chapman J, Fahey B, Gauthier ME, Mitros T, Richards GS, Conaco C, Dacre M, Hellsten U, et al. 2010. The *Amphimedon queenslandica* genome and the evolution of animal complexity. *Nature* 466:720–726.
- Suga H, Chen Z, de Mendoza A, Sebe-Pedros A, Brown MW, Kramer E, Carr M, Kerner P, Vervoort M, Sanchez-Pons N, et al. 2013. The *Capsaspora* genome reveals a complex unicellular prehistory of animals. *Nat Commun.* 4:2325.
- Tapon N, Harvey KF, Bell DW, Wahrer DC, Schiripo TA, Haber DA, Hariharan IK. 2002. *Salvador* promotes both cell cycle exit and apoptosis in *Drosophila* and is mutated in human cancer cell lines. *Cell* 110:467–478.
- Trapnell C, Pachter L, Salzberg SL. 2009. TopHat: discovering splice junctions with RNA-Seq. *Bioinformatics* 25:1105–1111.
- Trapnell C, Williams BA, Pertea G, Mortazavi A, Kwan G, Van Baren MJ, Salzberg SL, Wold BJ, Pachter L. 2010. Transcript assembly and quantification by RNA-Seq reveals unannotated transcripts and isoform switching during cell differentiation. *Nat Biotechnol.* 28:511–515.
- Wang K, Degerny C, Xu M, Yang XJ. 2009. YAP, TAZ, and Yorkie: a conserved family of signal-responsive transcriptional coregulators in animal development and human disease. *Biochem Cell Biol.* 87:77–91.
- Waterhouse RM, Zdobnov EM, Tegenfeldt F, Li J, Kriventseva EV. 2011. OrthoDB: the hierarchical catalog of eukaryotic orthologs in 2011. *Nucleic Acids Res.* 39:D283–D288.
- Wolff T, Ready DF. 1991. Cell death in normal and rough eye mutants of *Drosophila*. *Development* 113:825–839.

- Wu S, Liu Y, Zheng Y, Dong J, Pan D. 2008. The TEAD/TEF family protein Scalloped mediates transcriptional output of the Hippo growth-regulatory pathway. *Dev Cell*. 14:388–398.
- Xu T, Wang W, Zhang S, Stewart RA, Yu W. 1995. Identifying tumor suppressors in genetic mosaics: the *Drosophila lats* gene encodes a putative protein kinase. *Development* 121:1053–1063.
- Young SL, Diolaiti D, Conacci-Sorrell M, Ruiz-Trillo I, Eisenman RN, King N. 2011. Premetazoan ancestry of the Myc-Max network. *Mol Biol Evol*. 28:2961–2971.
- Zender L, Spector MS, Xue W, Flemming P, Cordon-Cardo C, Silke J, Fan ST, Luk JM, Wigler M, Hannon GJ, et al. 2006. Identification and validation of oncogenes in liver cancer using an integrative oncogenic approach. *Cell* 125:1253–1267.
- Zhang J, Ji J. Y., Yu M, Overholtzer M, Smolen GA, Wang R, Brugge JS, Dyson NJ, Haber DA. 2009. YAP-dependent induction of amphiregulin identifies a non-cell-autonomous component of the Hippo pathway. *Nat Cell Biol*. 11:1444–1450.
- Zhang L, Ren F, Zhang Q, Chen Y, Wang B, Jiang J. 2008. The TEAD/TEF family of transcription factor Scalloped mediates Hippo signaling in organ size control. *Dev Cell*. 14:377–387.
- Zhang X, Milton CC, Humbert PO, Harvey KF. 2009. Transcriptional output of the Salvador/warts/Hippo pathway is controlled in distinct fashions in *Drosophila melanogaster* and mammalian cell lines. *Cancer Res*. 69:6033–6041.
- Zhang Y, Liu T, Meyer CA, Eeckhoutte J, Johnson DS, Bernstein BE, Nusbaum C, Myers RM, Brown M, Li W, Liu XS. 2008. Model-based analysis of ChIP-Seq (MACS). *Genome Biol*. 9:R137.
- Zhao B, Kim J, Ye X, Lai ZC, Guan KL. 2009. Both TEAD-binding and WW domains are required for the growth stimulation and oncogenic transformation activity of yes-associated protein. *Cancer Res*. 69:1089–1098.
- Zhao B, Li L, Lei Q, Guan KL. 2010. The Hippo-YAP pathway in organ size control and tumorigenesis: an updated version. *Genes Dev*. 24:862–874.
- Zhao B, Tumaneng K, Guan KL. 2011. The Hippo pathway in organ size control, tissue regeneration and stem cell self-renewal. *Nat Cell Biol*. 13:877–883.
- Zhao B, Wei X, Li W, Udan RS, Yang Q, Kim J, Xie J, Ikenoue T, Yu J, Li L, et al. 2007. Inactivation of YAP oncoprotein by the Hippo pathway is involved in cell contact inhibition and tissue growth control. *Genes Dev*. 21:2747–2761.
- Zhao B, Ye X, Yu J, Li L, Li W, Li S, Lin JD, Wang CY, Chinnaiyan AM, et al. 2008. TEAD mediates YAP-dependent gene induction and growth control. *Genes Dev*. 22:1962–1971.